



10-2-12

EXPERIMENTAL STUDY ON DYNAMIC CHARACTERISTICS OF STRESS-RIBBON BRIDGE

Takao NAKAZAWA¹, Hajime TSUTSUMI² and Hiroshi YOKOTA¹

¹ Department of Civil Engineering, Miyazaki University,
Miyazaki, Japan

² Department of Civil Engineering, Kyushu University,
Fukuoka, Japan

SUMMARY

This paper describes the dynamic characteristics of stress-ribbon bridges obtained by experiments and theoretical analyses. It is revealed that the first natural frequency of the stress-ribbon bridge with a larger sag (20cm) is higher than one of the another (10cm). It is desirable that the amount of sag is designed to be larger in order to improve the dynamic characteristics of the bridge. The experimental results require us to develop a theoretical analysis taking account of the change of span length, caused by the change of contact length between stress-ribbon and saddle-like shaped support in the vibration.

INTRODUCTION

A stress-ribbon bridge is a very simple structure built by spanning of cables and lining them with reinforced concrete to provide the bridge with rigidities. Usually, the bridge of this type, which was proposed by Dr. Ulrich Finsterwalder in 1958 (Ref.1), does not require main towers, hangers and stiffening girders or frequent maintenance works. However, there are few bridges constructed for pedestrians in Japan and are little more than 10 in the world, because of less information on the dynamic characteristics of the bridge. Generally, stress-ribbon bridges have a low natural frequency, because the stress-ribbon is thin in comparison with its span length and has a low rigidity. Therefore, resonance may occur, if the natural frequency is the same as the frequency of walking behavior. The object of this paper is to investigate the dynamic characteristics of the stress-ribbon bridge, by model tests and theoretical analyses.

VIBRATION TESTS

Experimental bridges We made one-fifth models of a stress-ribbon bridge with span length of 50m, in order to investigate the effect of sag on the dynamic characteristics. Namely, we provided two experimental bridges with the same span length $L=10m$, width of 0.7m, and different sags of $s=10cm$ (Type-1) and $s=20cm$ (Type-2), as shown in Fig.1. Although we decided the thickness of the stress-ribbon as 10cm from the restriction of construction, this size may be rather a little thick for its span length.

Conditions for design are as follows: intensity of live load $=350kgf/m^2$ ($=245kgf/m$), drying shrinkage of concrete $=200 \times 10^{-6}$, creep coefficient of

concrete=2.6, range of temperature change= 20°C, allowable tensile force per a cable(T12.4)=9780kgf(ultimate tensile strength=16300kgf), and its relaxation coefficient =0.05. The cables of 8 in Type-1 and 5 in Type-2 were used, and their horizontal tensile forces were measured as Ho=22.6tf(Type-1) and Ho=11.2tf(Type-2) when their own weight was loaded. Photo.1 presents the experimental stress-ribbon bridges (Ref.2).

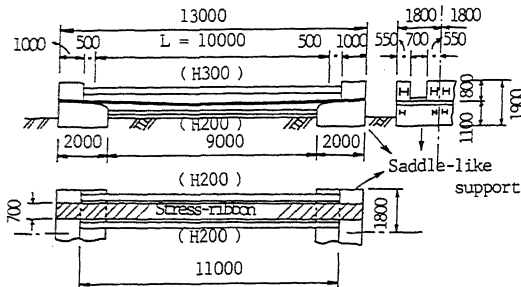


Fig. 1(a) Experimental Stress-Ribbon Bridge

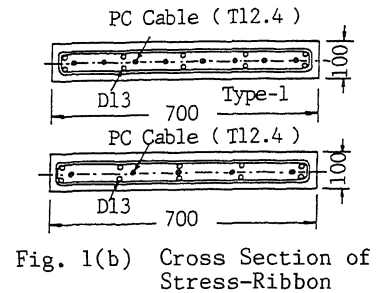


Fig. 1(b) Cross Section of Stress-Ribbon

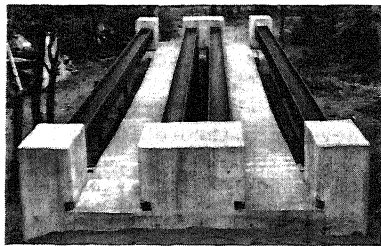


Photo 1 The Model Stress-Ribbon Bridges for Experiment (Left:Type-1, Right:Type-2)

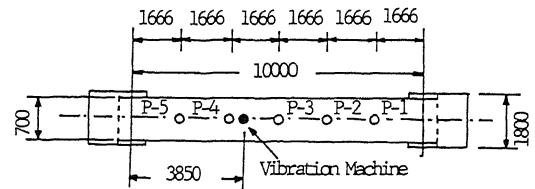


Fig. 2 Arrangement of Accelerometers and Vibration Machine

Method of experiments By means of vibration machine, vibration tests were conducted in vertical direction. In order to measure the vertical displacement of the bridge, we set up accelerometers and deflection seismographs at five points (P-1~P-5) having equal spaces on the stress-ribbon, as shown in Fig.2. We obtained the resonance curves about four stages of vibration force (150,300,450 and 600kgf), and estimated the damping constants.

FORMULA FOR ANALYSIS OF STRESS-RIBBON BRIDGE

Generally, the equation of motion for the system with many degrees of freedom can be written as follows:

$$F M \ddot{X} + X = 0, \quad (1)$$

where, F=flexibility matrix, M=inertia matrix, \ddot{X} =acceleration vector, X=deflection vector. Putting $X = \phi e^{i\omega t}$, Eq.(1) can be transformed as follows:

$$|I - \omega^2 F M| = 0, \quad (2)$$

where I=unit matrix. Giving F and M, natural circular frequency ω and vibration mode ϕ can be obtained.

Since the experimental stress-ribbons are rather a little thick for their span length, as above mentioned, the effect of flexural rigidity cannot be dis-

regarded. The flexibility matrix F can be obtained from the following deflection theory.

Now, assume that a stress-ribbon bridge with span length L forms a parabolic curve and that the cable is in horizontal equilibrium with H_0 , when its own weight q is loaded, as shown in Fig.3. By loading a concentrated load P at the distance, z, from the origin, the horizontal force changed into H_1 . The deflection of the stress-ribbon can be calculated from the following equation,

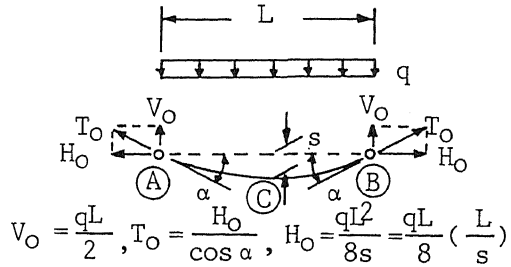


Fig. 3 Equilibrium of Stress-Ribbon

$$0 \leq x \leq z$$

$$y = \frac{PL}{H_1} \left[\frac{x}{L} \left(1 - \frac{z}{L} \right) - \frac{\sinh(k(L-z))}{kL \sinh(kL)} \sinh(kx) \right] - \frac{\Delta H}{H_0} \frac{qL^2}{H_1} \left[\frac{\cosh((kL/2)-kx)}{k^2 L^2 \cosh(kL/2)} - \frac{1}{k^2 L^2} + \frac{x(L-x)}{2L^2} \right],$$

$$z < x \leq L$$

$$y = \frac{PL}{H_1} \left[\frac{z}{L} \left(1 - \frac{x}{L} \right) - \frac{\sinh(kz)}{kL \sinh(kL)} \sinh(k(L-x)) \right] - \frac{\Delta H}{H_0} \frac{qL^2}{H_1} \left[\frac{\cosh((kL/2)-kx)}{k^2 L^2 \cosh(kL/2)} - \frac{1}{k^2 L^2} + \frac{x(L-x)}{2L^2} \right], \quad (3)$$

where, $H=H_1-H_0$, $k^2=H_0/EI$, E =Young's modulus of stress-ribbon, I =moment of inertia of stress-ribbon.

Therefore, if H_1 is given, the deflection can be obtained from Eq.(3). Regarding the change of temperature, we can calculate the increment of the horizontal force H and H_1 , from the following equation,

$$\frac{\Delta H}{EA} L \left(1 + 8 \frac{s^2}{L^2} \right) + \alpha \theta L \left(1 + \frac{16}{3} \frac{s^2}{L^2} \right) = \frac{PL}{H_1} \frac{8s}{L} \left[\frac{z}{2L} \left(1 - \frac{z}{L} \right) - \frac{1}{k^2 L^2 \sinh(kL)} \left\{ \sinh(kL) - \sinh(kz) - \sinh(k(L-z)) \right\} \right] - \frac{\Delta HL}{12H_1} \left(\frac{8s}{L} \right)^2 \left[1 - \frac{12}{k^2 L^2} + \frac{24}{k^3 L^3} \tanh\left(\frac{kL}{2}\right) \right], \quad (4)$$

where, α =coefficient of liner expansion, θ =change of temperature, A =sectional area of stress-ribbon. From Eqs.(3) and (4), we can obtain F matrix.

RESULTS AND DISCUSSION

Figs.4(a),(b) and (c) show the resonance curves at the point P-3 generated by the vibration forces of 300, 450 and 600kgf(at 10Hz), respectively. The resonance curves of Type-1 and Type-2 are designated by symbols \bullet and Δ , respectively. Fig.5 shows the natural frequencies corresponding to the change of vibration forces and the vibration modes. From this figure, it is seen that the frequency of the 1st-axis-symmetric mode slightly increases in case of large vibration force, like as hardening type. The reason of this matter may be that the contact length between the stress-ribbon and saddle-like shaped support gets longer when the stress-ribbon moves down, namely, the span length is relatively shortened. The frequencies of the 1st-point-symmetric and 2nd axis-symmetric modes significantly decrease as the vibration forces get stronger. Although a cable has a higher frequency as the tensile force get stronger, it is seen from Fig.5 that the frequency of 1st-axis-symmetric mode of Type-2, having a relatively large sag, is higher than one of Type-1. This may be caused by the difference of their rigidities owing to the different amount of sag.

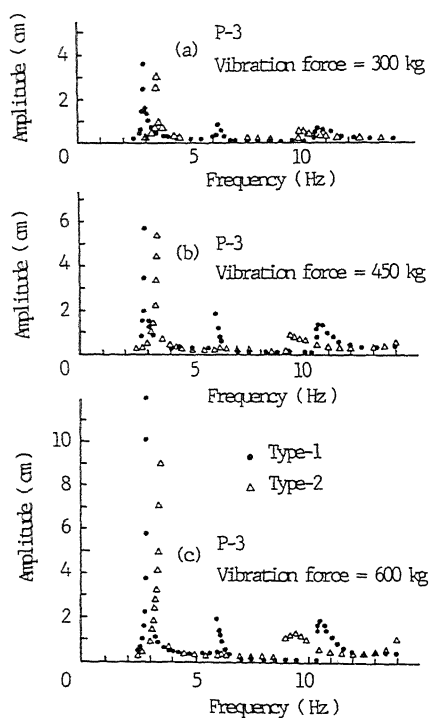


Fig. 4 Resonance Curves

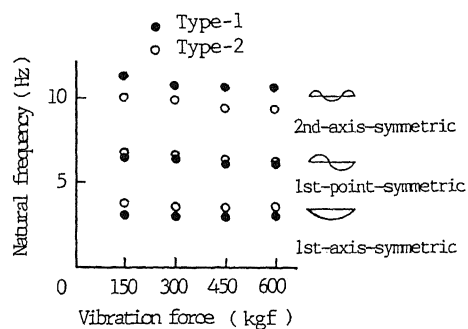


Fig. 5 Natural Frequency versus Vibration Force

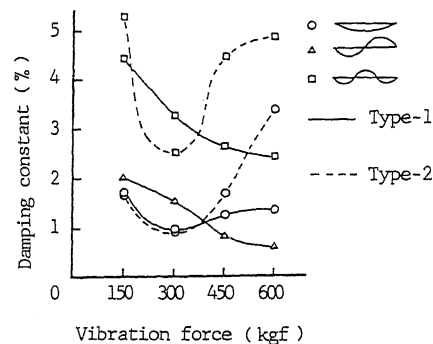


Fig. 6 Damping Constants versus Vibration Force

From Fig.4, it can be seen that the amplitude of the 1st-axis-symmetric mode is the largest in both bridges. While, in the case of Type-1, the amplitude of the 1st-point-symmetric mode is smaller than one of the 2nd-axis symmetric mode, although we presupposed that the amplitudes became smaller in order of modes; 1st-axis-symmetric, 1st-point-symmetric and 2nd-axis-symmetric modes. The resonance curves of 1st-point-symmetric and 2nd-axis-symmetric modes show the shape of softening type that immediately raise at their own

resonances. Fig.6 shows the damping constants obtained from the above curves.

Fig.7 shows the relationship between natural frequencies f and the ratio of sag to span, s/L . From this figure, for Type-1 ($s/L=0.01$), the 1st-axis-symmetric, 1st-point-symmetric and 2nd-axis-symmetric modes of vibration appear in order of the natural frequency. The order of these modes is common among the results by the theoretical analysis, the calculation using the flexibility matrix obtained through the experiment, the experiment by using a vibration machine, and the experiment by the jumping of one person (70kgf) at the middle of span. Also, their natural frequencies are well in agreement as a whole.

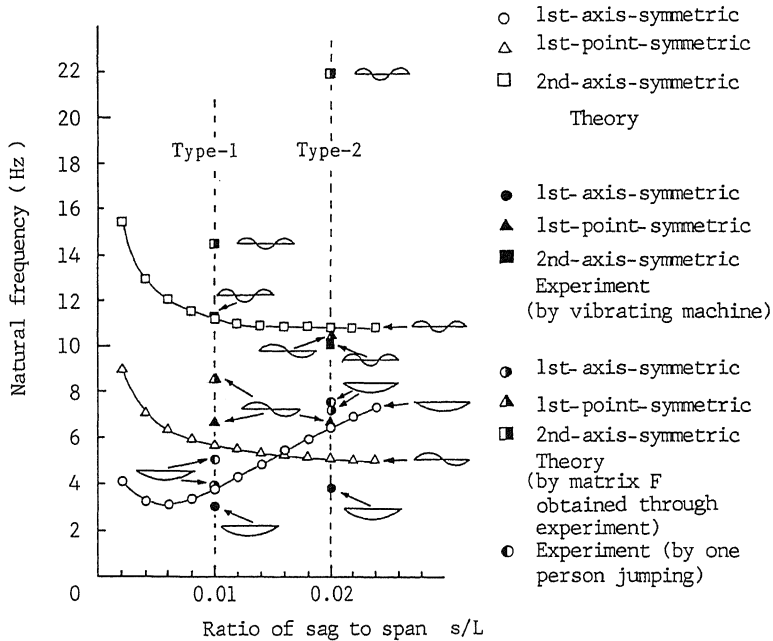


Fig. 7 Influence of Ratio of Sag to Span on Natural Frequency

For Type-2 ($s/L=0.02$), the order of modes of vibration derived from the experiment using the vibration machine agree with the one of Type-1. However, in the theoretical analysis, 1st-axis-symmetric and 1st-point-symmetric modes occur in reverse order. Their frequencies are different from ones of the experiment. While, the natural frequency of 1st-axis-symmetric mode agrees with ones obtained from the experiment by jumping of one person and the calculation by using the flexibility matrix estimated through experiment, as a whole. Anyway, for Type-2, there are differences of the natural frequencies and modes between the theoretical and experimental

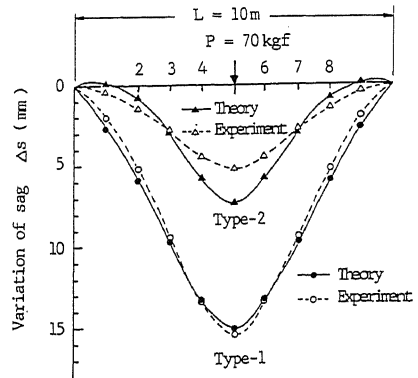


Fig. 8 Deflection Curves

results. These are caused by the difference of the deflection curves derived from the theoretical analysis and the experimental ones, as shown in Fig.8, which shows the deflection curves obtained from Eq.(3) and the experiments when the concentrated load of 70kgf is loaded at the middle of span. It can be presumed that the span length in the theoretical analysis is different from one in the experiment, due to the change of the contact length between the stress-ribbon and the saddle-like shaped support. Namely, although the span length is significantly changed in reality, it is assumed to be constant in the theoretical analysis.

CONCLUSIONS

The dynamic characteristics of stress-ribbon bridge are influenced considerably by the amount of sag, tensile force of cable, and the length of contact between the stress-ribbon and saddle-like shaped support. Especially, it is necessary to develop a theoretical analysis taking account of the change of span length caused by vibration.

The other results are summarized as follows:

- 1) It is obtained that the first natural frequency of the stress-ribbon bridge with a larger sag (Type-2:20cm) is higher than one of the another (Type-1:10cm) from our experiments. This is also revealed by the theoretical analysis although the vibration modes are different.
- 2) It is desirable that the amount of sag is designed to be larger to improve the dynamic characteristics as long as pedestrians do not feel fatigue to walk.
- 3) It is revealed that the third natural frequency decreases correspondingly to the amount of sag, by the experimental results and theoretical analysis.
- 4) The experiments give us interest resonance curves such as the shape of hardening type for the first natural frequency and the shapes of softening type for the second and third natural frequencies, respectively.

ACKNOWLEDGMENTS

We would like to express our gratitude for the guidance received from Dr. Yoshimaru MURAKAMI, formerly professor of Miyazaki university, and the assistances received from Miyazaki prefecture office and Sumitomo Construction Company.

REFERENCES

1. Finsterwalder, U., Festschrift Ulrich Finsterwalder 50 Jahre für DYWIDAG, Verlag G.Brau, Karlsruhe, (1973).
2. Murakami, Y., Nakazawa, T. and Sezaki, M., Model Tests and Analyses on the Pedestrian Suspended-Slab Bridges, Proceedings of the Recent Advance in Structural Engineering, Japan-Thai Civil Engineering Conference, Bangkok, Thailand, (1985).